Journal of Non-Crystalline Solids 398–399 (2014) 57–61

Contents lists available at ScienceDirect

Journal of Non-Crystalline Solids

journal homepage: www.elsevier.com/ locate/ jnoncrysol

Structural, thermal and optical properties of CaBO and CaLiBO glasses doped with Eu^{3+}

S.S. Rojas [a,*], J.E. De Souza [a], K. Yukimitu [b], A.C. Hernandes [c]

[a] Laboratório de Materiais Cerâmicos Avançados, Faculdade de Ciências Exatas e Tecnologia, Universidade Federal da Grande Dourados — UFGD, CP 364, 79804-970 Dourados, MS, Brazil
[b] Grupo Vidros e Cerâmicas, Departamento de Física e Química, Universidade Estadual Paulista — UNESP, 15385-000 Ilha Solteira, SP, Brazil
[c] Grupo Crescimento de Cristais e Materiais Cerâmicos, Instituto de Física de São Carlos, Universidade de São Paulo — USP, CP 369, 13560-970 São Carlos, SP, Brazil

ARTICLE INFO

Article history:
Received 25 October 2013
Received in revised form 16 April 2014

Keywords:
Glasses;
Borate glasses;
FT-IR;
Thermal properties;
CaLiBO glass

ABSTRACT

Thermal, structural and optical properties of undoped and Eu^{3+} doped CaBO and CaLiBO glasses were carried out by the Raman, FT-IR, UV–Vis absorption, fluorescence, thermoluminescence and DSC analyses. The addition of Li^{+} to the CaBO glass changes its characteristic temperatures by decreasing the glass transition, T_g, and melting temperatures to about 40 °C and 50 °C, respectively, due to a M–O interaction (M = modifier cation) that plays an important role in determining T_g. Moreover, a liquid–liquid phase separation observed in the binary system was avoided after Li^{+} addition, which allows the melting of glasses in lower temperatures (from 1450 °C to 1100 °C). In spite of the variations on thermal properties, small changes in the glass structure concerning boron–oxygen arrangements were seen by the Raman and FT-IR when compared to the spectra obtained from all prepared samples (variations < 10% in the relative area of Gaussian peaks) and were understood in terms of an isomerization reaction among the structural units into the glass network. Also important is that CaBO and CaLiBO glass matrices have a high transparency in the UV region ($\lambda_{cut\text{-}off}$ < 190 nm) and this fact in combination with thermal, optical and structural characteristics indicates their high potential for optical applications.

1. Introduction

Rare-earth (RE) doped borate glasses present interesting properties which allow their use in different applications, such as new phosphor materials, fluorescent display devices, radiation detection sensors, optical fibers, as well as, solid-state lasers [1–5]. Calcium borate glasses, particularly in the composition of calcium tetraborate CaB_4O_7, are very attractive to evaluate the effects of chemical environment on the optical properties of RE ions by presenting low melting temperature, high thermal stability and no hygroscopicity [5]. Furthermore, beyond the fact that borate glasses are advantageous materials for application in radiation dosimetry, they still have an effective atomic number close to that of the human tissue (Z_{eff} = 7.42) [5,6]. Previously, we reported about the thermoluminescence (TL) of Dy^{3+} and Li^{+} co-doping calcium borate glass and glass-ceramics that shows an intrinsic TL emission under UV exposure [5,6]. This TL sensitivity is dependent on the trivalent RE dopant, which may form complex defects in borates by creating hole or electron trap centers depending on the boron–oxygen arrangement in the glass structure [6]. Moreover, the structure of borate glasses is very interesting due to the widely known "boron anomaly phenomenon", i.e., the coordination changes of the network forming cations in the glass structure that provide a maximum behavior in several properties, such as thermal expansion coefficient, viscosity, glass transition temperature and others [7,8].

The behavior concerning the glass formation and its structural order, by considering the local and medium range, is important to understand how glass structure relates to its physical properties. It is known from the literature that alkali borate glasses in the binary system $xM_2O \cdot (1-x)B_2O_3$ (M = alkali metal ion) have a dependence to their properties with the type of alkali metal [9–12]. For example, a possible explanation to the dependence between M and the glass transition temperature T_g is made by the co-existence of both metaborate triangles and tetrahedral units that promoted the isomerization reaction: $B\varnothing_4^- \Leftrightarrow B\varnothing_2O^-$, which determines the local and medium range order structure of glasses in compositions below x ≈ 0.30 [9–11].

Presently, Eu^{3+} ions have shown a preferred dopant for borates, by presenting a high fluorescence efficiency of the transition $^5D_0 \rightarrow {}^7F_2$ (orange-red region) and a spectrum very sensible to small changes in its chemical surroundings, turning possible their application as sensors [1,2,12]. Some studies have shown that the red/orange fluorescence intensity ratio reaches a maximum as a function of alkali earth addition to the glass composition [1,2]. In the case of calcium borate glasses containing barium oxide, it was observed that the fluorescence intensity of Eu^{3+} is enhanced up to 10 mol% of BaO content, and decreases to higher concentrations [1,2].

* Corresponding author.
E-mail addresses: seilarojas@gmail.com (S.S. Rojas), hernandes@if.sc.usp.br (A.C. Hernandes).

http://dx.doi.org/10.1016/j.jnoncrysol.2014.04.026
0022-3093/

Therefore, the goal of the present work is to evaluate the thermal, structural and optical properties of the undoped CaB_4O_7 and CaB_4O_7 containing Li^+ glasses after doped with Eu^{3+} by means of X-ray diffraction (XRD), differential scanning calorimetry (DSC), Raman, Fourier transform infrared spectroscopy (FT-IR), ultraviolet–visible optical absorption (UV–Vis), fluorescence spectroscopy and thermoluminescence (TL) techniques. Hereafter the glass matrix containing Li^+ is referred to as CaLiBO ($90CaB_4O_7$–$10Li_2O$ mol%), while CaB_4O_7 is referred to as CaBO.

2. Experimental

High-purity powders of B_2O_3 (Alfa Aesar — 99.98%), $CaCO_3$ (Alfa Aesar — 99.95%), $LiCO_2$ (Alfa Aesar — 99.99%), and Eu_2O_3 (Sigma Aldrich — 99.99%) were adequately weighed (Mettler Toledo AE 163, ±0.1 mg) in the required molar fraction presented in Table 1.

Batches of 20 g of reagents were melted in a pure platinum crucible (Heraeus Vectra — 99.9%) at temperatures ranging from 1100 °C to 1450 °C, depending on the composition. The temperatures used during the melting process were referred to as *MT* and are presented in Table 1. The preparation process of CaBO glass is described in more details in a previous work [5].

The amorphous nature of the glass samples was confirmed by XRD in a Rigaku Diffractometer — model Ultima IV, at 40 kV and 40 mA, with Cu $K\alpha_1$ radiation (results not shown herein).

The densities of the samples were obtained by applying the fluid displacement method – Archimedes' principle [7,8] – with distilled water as the immersion liquid at room temperature ($\rho = 0.997$ g/cm^3 at 25.0 ± 0.2 °C) by using a digital balance Mettler Toledo AG 285, sensitive to 0.1 mg. Three different pieces of each glass sample were used to determine its density value.

Thermal analysis was carried out by DSC using a Netzsch STA 409C, in Al_2O_3 pans, synthetic air (80% N_2 and 20% O_2) as atmosphere and 10 °C/min of heating rate.

Raman scattering was performed at room temperature in the wavenumber range from 200 to 1800 cm^{-1} with a confocal Raman microscope WiTec, model Alpha 300S — A/R. Samples were excited with a 514.5 nm air-cooled Ar ion laser (Melles Griot, model 35-LAL — 515-230). In addition, infrared absorption measurements were done by Attenuated Total Reflectance (ATR) spectroscopy in a Bruker Vertex 70 FT-IR spectrometer. The experimental conditions were 100 scans and 4.0 cm^{-1} of resolution, within the range from 600 up to 4000 cm^{-1}.

The UV–Vis absorption spectra were collected in the range from 190 to 1000 nm in a Cary 50 (Varian) spectrometer, using 1 mm thick samples. Fluorescence measurement of Eu^{3+} doped glasses was recorded at room temperature by using a portable spectrofluorometer (MM Optics) which consists of a laser operating at 405 nm or 532 nm, a monochromator, a Y-type optical fiber, and a portable computer.

Thermoluminescence measurements were done in a Harshaw Model 3500 TL Analyzer, by using glass powders (~3 mg) without previous thermal annealing. Irradiation was performed at room temperature with an UV light (500 W Hg lamp), which emits mainly in the spectral range between 254 and 365 nm, and provides an evaluated light beam irradiance of 7.2 mW/cm^2, at a distance of 30 cm from the samples. The UV irradiation was kept for 20 min with no external light filters. The linear heating rate was set at 5 °C/s and all measurements were taken in N_2 atmosphere, in order to avoid spurious TL signals [6,13]. Light emission was recorded over the temperature range from 50 °C up to 400 °C. The TL curves were obtained by averaging three measurements and the error bars are associated to variation in weight of the samples.

3. Results and discussion

To avoid liquid–liquid phase separation in the preparation of binary CaO–B_2O_3 glasses high temperatures are required in order to obtain a homogeneous melt [5,14,15]. In this work, the addition of 10 mol% of Li_2O to the CaB_4O_7 glass composition prevents this liquid–liquid phase separation by allowing the preparation of glasses at much lower temperatures, as can be noted in *MT* values in Table 1.

Table 1 also presents the density data obtained by the Archimedes' method and summarizes the thermal parameters obtained from the DSC measurements, whose curves are shown in Fig. 1. As can be seen from the results, the addition of 10 mol% of Li_2O to the CaBO composition causes significant changes in the characteristic temperatures of the glass without causing a significant variation in density values. After the addition of 1 mol% of Eu_2O_3 an increase in density values of CaBO and CaLiBO matrices was observed as a consequence of its higher molecular mass than that observed in B_2O_3, CaO or Li_2O compounds. Despite the fact that Eu_2O_3 promoted an increase in density of the CaBO and CaLiBO glasses, its addition does not affect their glass transitions (T_g). In contrast, the lithium oxide was expected to act as a glass network modifier, since its incorporation into the glass lattice breaks up the glass network and consequently reduces the glass transition temperature. In fact, the lithium oxide addition to the CaBO glass caused an expressive decrease in T_g and T_m values, by about 40 °C and 50 °C, respectively.

Thermal characteristics of the glasses were evaluated by three thermal parameters: i) $\Delta T = T_x - T_g$, being T_x the onset of crystallization, implies the glass stability against devitrification; ii) $K_H = \frac{T_c - T_g}{T_m}$ (Hrüby's parameter) and iii) $K_W = \frac{T_c - T_g}{T_m}$ (Weinberg's parameter), by considering T_c as the maximum of crystallization, are associated to the glass stability against crystallization on heating and can also be correlated to the glass forming ability [16,17]. As larger the K_H, or K_W parameter, the higher the glass stability on heating [17]. The studied glasses present high thermal stability against devitrification, observed by the ΔT values, that varies from 129 °C up to 145 °C. Considering the cited parameters, the CaLiBO:Eu sample presents the best thermal stability among the studied glasses.

In order to get some insight about the glass structure, Raman and ATR analyses were performed and the vibration bands were decomposed in multiple Gaussian peaks, as shown in Fig. 2. Further analysis on the structural arrangement of boron–oxygen in the glass structure was done by considering the relative area of each Gaussian fit obtained from both Raman and ATR spectra (see Fig. 3). The assignments to Raman and IR vibrations were summarized in Table 2. A number of eight bands were identified by decomposition of Raman spectra and were coincident to the attribution done by different researchers at

Table 1
Melting temperature, *M*, adopted int the glass preparation process, density and thermal stability parameters obtained from DSC curves.

Sample	Nominal composition (mol%)	*MT* (°C)	Density (g/cm^3)	Thermal parameters						
				T_g (±2 °C)	T_x (±2 °C)	T_c (±2 °C)	T_m (±2 °C)	ΔT (±4 °C)	K_H	K_w
CaBO	CaB_4O_7[a]	1450	2.56 ± 0.02	648	777	800	890	129	1.68 ± 0.05	0.13 ± 0.02
CaBO:Eu	$99CaB_4O_7$:$1Eu_2O_3$	1200	2.66 ± 0.02	647	782	800	884	135	1.82 ± 0.05	0.13 ± 0.03
CaLiBO	$90CaB_4O_7$–$10Li_2O$	1100	2.57 ± 0.03	606	733	752	840	127	1.66 ± 0.05	0.13 ± 0.03
CaLiBO:Eu	$89CaB_4O_7$–$10Li_2O$:$1Eu_2O_3$	1100	2.63 ± 0.02	606	751	773	820	145	3.55 ± 0.08	0.15 ± 0.02

[a] CaB_4O_7 corresponds to $33.33CaO$–$66.67B_2O_3$ mol% composition.

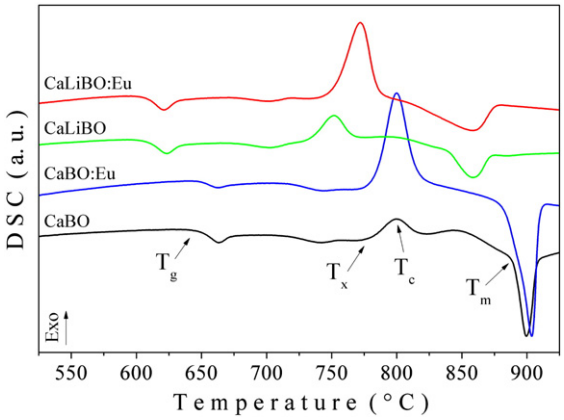

Fig. 1. DSC curves of glass samples. The characteristic temperatures T_g, T_x, T_p and T_m are indicated by arrows.

the literature [18–22]. Experimental Raman spectra of all glasses presented a high intense band centered at ~770 cm^{-1} that corresponds to the symmetric breathing in rings with one B∅$_4$ unity associated to pentaborate ($B_5O_{10}^-$) structural groups (∅ = bridging oxygen; O^- = non-bridging oxygen). This attribution was based on the work published by Maniu and co-workers [20], who stated that glasses with low CaO content present pentaborate groups and not tetra- or triborates. However, a major relative area (among 20 to 30%) of Raman vibration was observed in the band centered at approximately 720 cm^{-1} which is attributed to the B–∅–B stretching in metaborate

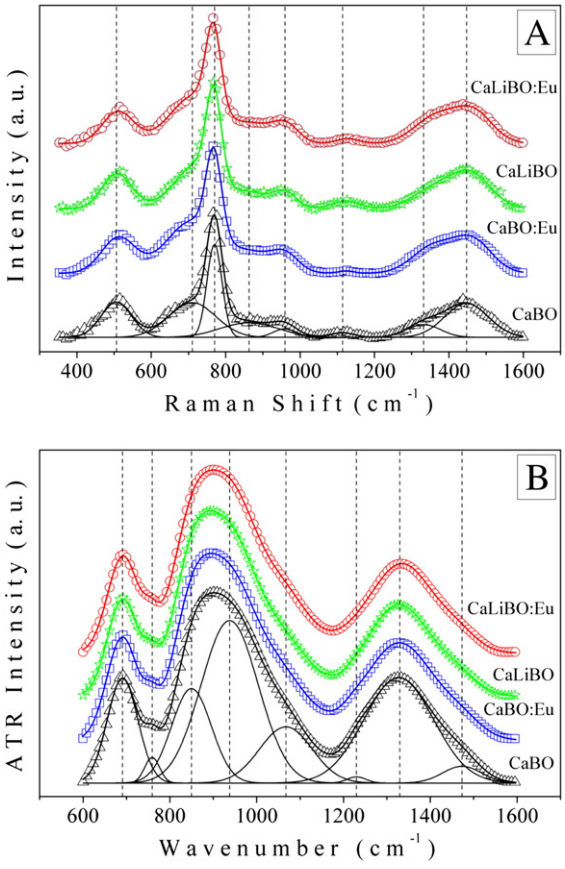

Fig. 2. Micro-Raman (A) and ATR (B) absorption spectra of the bulk glasses. Example of Raman and ATR spectra decomposition obtained from CaBO sample (multiple Gaussians fit). Symbols represent the experimental data and the solid lines are the fitted curves. Dashed vertical lines are only guide for eyes.

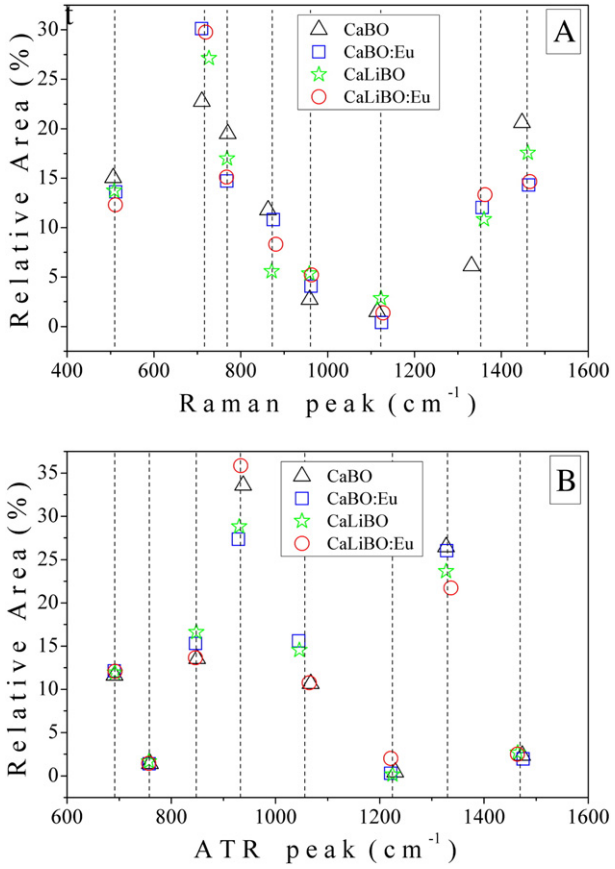

Fig. 3. Relative area of decomposed bands (multiple Gaussian peaks) from the micro-Raman (A) and ATR (B) spectra. Dashed vertical lines are only guide for eyes.

chains (B_3 ∅ $_4O_3^{3-}$) [18–20]. Small differences among the micro-Raman spectra of the glasses, concerning variations <10% in the relative area of the peaks, were observed to be ~720 cm^{-1}, ~1363 cm^{-1} and ~1463 cm^{-1} wavenumbers. These two last bands were attributed to Raman shift due to stretching in B∅$_2$O$^-$ linked to B∅$_4$ unit and [B∅$_2$O]$^-$ triangles in chain-type arrangements, respectively [21]. The band vibration at ~882 cm^{-1} was attributed to B–∅–B stretching in pyroborate (B_2 ∅ O_4^{4-}) units [18,19,21]. According to Maniu et al. [20], pyroborate groups are present in small number from low to high CaO content, but they can still be detected by Raman spectroscopy. Santos et al. [18] observed the formation of pyroborate units for glass at $4Y_2O_3$–32CaO–$64B_2O_3$ mol% composition by Raman spectroscopy. Thus, we may suppose that this overmodified structure is beginning to be formed in the glass structures for the samples prepared herein.

Mid-infrared absorption of different borate glasses is typically observed in three wavenumber regions. The band around 700 cm^{-1} is related to the bending vibration of B–∅–B linkage in the borate network [11,22]. Vibrations between 800 and 1150 cm^{-1} are due to the groups formed by B∅$_4$ and B∅$_3$ without the formation of non-bridging oxygen, and finally, between 1150 and 1550 cm^{-1} the vibrations from the stretching of B–∅ and B–O$^-$ in B∅$_3$ and B∅$_2$O$^-$ units are found [22]. As expected, ATR spectra of the present glasses were characterized by three broad and intense bands centered at approximately 691 cm^{-1}, 900 cm^{-1} and 1330 cm^{-1}. No bands were observed in the 3000–4000 cm^{-1} region in which hydroxyl groups have their characteristic vibrations (for convenience, the range from 1600 cm^{-1} up to 4000 cm^{-1} was omitted in the spectra of Fig. 2–B). After decomposition of ATR spectra in multiple Gaussian peaks, a number of eight bands were identified and attributed in accordance to the references [1,5,11,21,22]. The main band vibration, that presents the major relative area, was observed at ~933 cm^{-1} and it was indexed as the B–∅ stretching of BO_4^- in diborate

Table 2
Vibrational wavenumber of borate groups observed in the Raman and IR spectra of glasses.

Raman attribution		IR attribution	
Peak position (cm^{-1})	Assignment	Peak position (cm^{-1})	Assignment
~509	B–∅–B stretching in BO_4^- units	~691	B–∅–B bending vibration in borate rings
~722	B–∅–B stretching in metaborate chains	~756	B–∅ stretching of BO_4^- in metaborate chains and rings
~769	Symmetric breathing in rings with one $B\varnothing_4$ unit (pentaborate)	~848	B–∅ stretching of BO_4^- in tri-, tetra- and pentaborate groups
~882	B–∅–B stretching bridges in pyroborate units	~933	B–∅ stretching of BO_4^- in diborate groups
~962	B–∅–B stretching in BO_4^- units	~1055	B–∅ stretching of BO_4^- in pentaborate groups
~1122	B–O^-/B–∅–B stretching in diborate units	~1224	B–∅ stretching of $[B\varnothing_2O^-]_n$ in metaborate chains
~1363	BO_2^- linked to BO_4 unit	~1330	B–O^- stretching of BO_3 unit in metaborate,
~1463	$[BO_2]^-$ triangles in chain-type arrangements	~1470	B–O^- stretching of $[B\varnothing_2O^-]_n$ in metaborate chains or antisymmetrical stretching of B–O^- in BO_3^{3-}

($B_4O_9^{2-}$) groups. The second one was observed at ~1330 cm^{-1} and attributed to the B–O^- stretching of BO_3 unit in metaborate groups. Despite the great similarity among the ATR spectra, small differences in the relative area of peaks (<10%) were mainly observed at ~933 cm^{-1} and ~1055 cm^{-1}, the last vibration represents the B–∅ stretching of BO_4^- in pentaborate groups.

It was reported in the literature that CaLiBO glasses present an independence of glass structure on rare-earth ions [1]. In the present work, very small changes in the boron–oxygen arrangements in CaBO glass structures after Eu^{3+} or Li^+ addition were only possible to be observed after decomposition of the micro-Raman and ATR experimental curves. The Li^+ addition to the glass structure causes a significant reduction in the glass transition temperature but no significant changes (<10% in the area of peaks) in the boron–oxygen arrangements could be confirmed by Raman and IR measurements. As proposed by Yiannopoulos and coworkers [9], our results may be explained by a combined effect of Li–O and B–O interactions, since the Li^+ ion provides a lower crosslinking efficiency when compared to Ca^{2+} that exhibits a higher coordination number with oxygen atoms in the glass network, while the small changes observed in the Raman and IR spectra may be understood by the isomerization reaction $B\varnothing_4^- \Leftrightarrow B\varnothing_2O^-$.

Fig. 4 presents the UV–Vis absorption spectra of Eu^{3+} doped and undoped CaBO and CaLiBO glasses. The undoped CaBO and CaLiBO glasses presented identical spectra with very high transparency in the UV region. Only for comparison, the cut-off (absorption edge) obtained from the CaBO and CaLiBO glass matrices ($\lambda_{cut\text{-}off} < 190$ nm) was similar to that obtained from pure and doped lithium tetraborate single crystals [23]. The doped glasses have shown a shift in their cut-off wavelength to higher values, being 271 nm and 277 nm for CaBO:Eu and CaLiBO:Eu, respectively. According to the inset in Fig. 4, eleven characteristic bands of Eu^{3+} absorption were identified and they are listed in Table 3 [1,24]. A

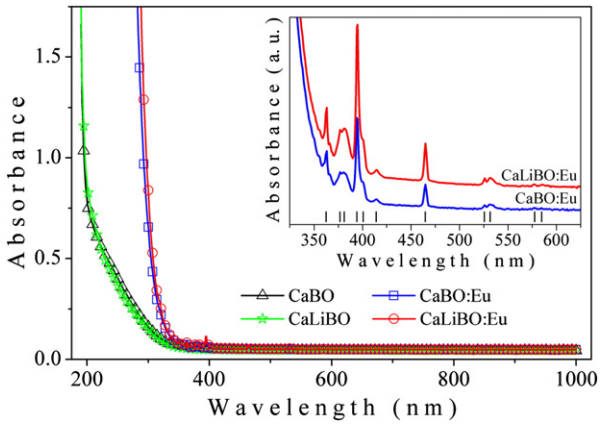

Fig. 4. Optical absorption spectra of Eu^{3+} doped and undoped CaBO and CaLiBO glasses.

higher intensity absorption was observed in the $^7F_0 \rightarrow {}^5L_6$ transition (at ~394.5 nm) while a very low intensity was observed in the $^7F_0 \rightarrow {}^5D_0$ transition (at ~577.5 nm) which is explained by considering the selection rule for induced electric dipole transition ($\Delta J = 0 \pm 1$) [1].

Fluorescence of Eu^{3+} doped glasses was carried out by excitation both at 405 and 532 nm which resulted in identical spectra that differ only in intensity, this being about three orders of magnitude higher when exciting with the more energetic radiation. Fig. 5 presents the spectra obtained from CaBO:Eu and CaLiBO:Eu excited at 405 nm. The radioactive emissions were related to five transitions at $^5D_0 \rightarrow {}^7F_0$, $^5D_0 \rightarrow {}^7F_1$, $^5D_0 \rightarrow {}^7F_2$, $^5D_0 \rightarrow {}^7F_3$ and $^5D_0 \rightarrow {}^7F_4$, that were directly identified in Fig. 5. A higher emission intensity was observed in the $^5D_0 \rightarrow {}^7F_2$ transition (orange region) that occurs at 615.4 nm in CaBO:Eu and also in CaLiBO:Eu glasses, being of highest intensity to the last one. Only for comparison, this transition is known to occur at 610 nm to 612 nm in phosphate, silicate and tellurite glasses [1]. The red-to-orange fluorescence intensity ratio for Eu^{3+} ions, well known as R/O factor, is defined as the ratio of integrated emission intensity of the $^5D_0 \rightarrow {}^7F_2$ to $^5D_0 \rightarrow {}^7F_1$ transition. The R/O factor is related to the local asymmetry and covalence bonding between lanthanide ions and its nearest surrounding. The R/O factors obtained from the CaBO:Eu^{3+} and CaLiBO:Eu^{3+} glass samples were 3.4 and 3.3, respectively. This small difference in R/O factor (by about 3%) implies a little decrease in the asymmetry and covalence of Eu^{3+} ions to CaLiBO in comparison to the CaBO glass and corroborate with no significant changes in the glass structure observed by the Raman and FT-IR experiments.

Thermoluminescence measurements were done in order to investigate the influence of Eu^{3+} and Li^+ addition to the generation of defects (electron or hole trap centers) responsible for the TL emission in calcium borate glass, turning it possible a comparison among the TL efficiency of the different glass samples. Fig. 6 shows the TL glow curves obtained from all samples after 20 min of exposure to a UV source. The results obtained herein have shown an intense and broad TL emission from undoped CaBO glass with a maximum at ~182 °C. The addition of Li^+

Table 3
Absorption bands of Eu^{3+} obtained from CaBO and CaLiBO glasses.

	Energy (cm^{-1})	Wavelength (nm)
$^7F_0 \rightarrow {}^5D_4$	27,579	362.6
$^7F_0 \rightarrow {}^5D_4$	26,525	377.0
$^7F_0 \rightarrow {}^5G_2$	26,219	381.4
$^7F_0 \rightarrow {}^5L_6$	25,348	394.5
$^7F_1 \rightarrow {}^5L_6$	24,944	400.9
$^7F_1 \rightarrow {}^5D_3$	24,131	414.4
$^7F_0 \rightarrow {}^5D_2$	21,505	465.0
$^7F_0 \rightarrow {}^5D_1$	19,011	526.0
$^7F_0 \rightarrow {}^5D_1$	18,815	531.9
$^7F_0 \rightarrow {}^5D_0$	17,316	577.5
$^7F_0 \rightarrow {}^5D_0$	17,076	585.0

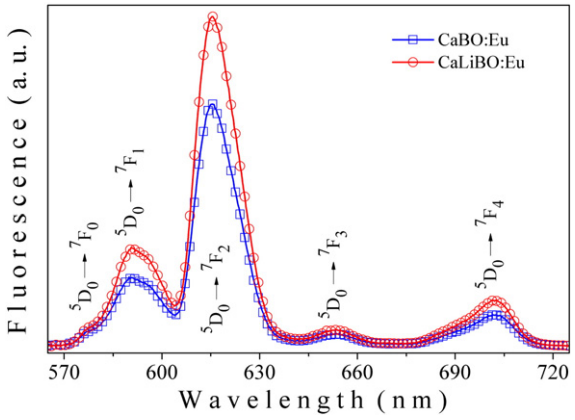

Fig. 5. Fluorescence spectra of Eu^{3+} doped CaBO and CaLiBO glasses. Laser excitation at 405 nm.

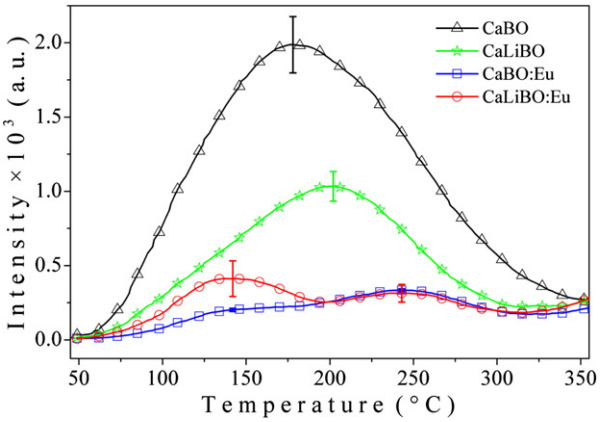

Fig. 6. TL glow curves obtained from glasses under 20 min of UV irradiation.

to CaBO composition has shifted the maximum of emission to higher temperatures, ~202 °C, but decreased its TL intensity by about 2 times. After Eu^{3+} doping both glass matrices, the intensity of TL glow curve has become smaller and two temperatures of maximums became visible, the first one at ~142 °C and the second one at ~243 °C. The observed decrease in the TL signal after Li^+ and Eu^{3+} additions may be understood by a reduction in the number of defects responsible for the TL emission.

4. Conclusions

Some physical properties of calcium tetraborate glasses prepared by the melting molding method were evaluated on thermal, optical and structural characteristics of the samples. We have observed that the addition of 10 mol% of Li_2O and 1 mol% of Eu_2O_3 to the calcium tetraborate glass (CaB_4O_7) causes very small changes to the non-crystalline structure as confirmed by Raman and IR spectroscopies, that was explained by the isomerization reaction: $B\varnothing_4^- \Longleftrightarrow B\varnothing_2O^-$. Nevertheless, lithium oxide presents an expressive influence on the characteristic temperatures of glasses, by decreasing T_g and T_m temperatures and by preventing a liquid–liquid phase separation commonly observed in the binary $CaO–B_2O_3$ system which allowed to obtain a more thermally stable and no hygroscopic sample with structure characteristics very similar to that observed in CaB_4O_7 tetraborate glass. The effect of Li^+ on the characteristic temperatures of the glasses may be understood in terms of the Li – O bonding interaction, since the monovalent ions, Li^+, produce lower crosslinking efficiency when compared to the divalent, Ca^{2+} ion. Thermoluminescence was greatly affected by the Li^+ and mainly by the Eu^{3+} addition that promoted a significant decrease in the number of generated defects responsible for the TL emission. On the other hand, the possibility of doping these matrices with trivalent rare-earth ions opens up interesting viewpoints in terms of optical devices by combining the excellent transparency of these glasses in the UV region ($\lambda_{cut\text{-}off} < 190$ nm) with their excellent thermal stability and structural characteristics.

The authors gratefully acknowledge the financial support of the Brazilian agencies CNPq, Fundect (Process number 23/200.667/2012), FAPESP and CAPES.

References

[1] G. Tripathi, V.K. Rai, S.B. Rai, Opt. Commun. 264 (2006) 116–122.
[2] V.K. Rai, A. Rai, Appl. Phys. B 86 (2007) 333–335.
[3] G. Tripathi, V.K. Rai, S.B. Rai, Appl. Phys. B 84 (2006) 459–464.
[4] V.K. Rai, C.B. Araujo, Spectrochim. Acta A 69 (2008) 509–512.
[5] S.S. Rojas, K. Yukimitu, A.S.S. Camargo, L.A.O. Nunes, A.C. Hernandes, J. Non-Cryst. Solids 352 (2006) 3608–3612.
[6] S.S. Rojas, K. Yukimitu, A.C. Hernandes, Nucl. Instrum. Methods 266 (4) (2008) 653–657.
[7] A.K. Varshneya, Fundamentals of Inorganic Glasses, Society of Glass Technology, New York, 2006.
[8] J.A. Shelby, Introduction to Glass Science and Technology, The Royal Society of Chemistry, Alfred, 1997.
[9] Y.D. Yiannopoulos, G.D. Chryssikos, E.I. Kamitsos, Phys. Chem. Glasses 42 (2001) 164–172.
[10] C.P. Varsamis, E.I. Kamitsos, G.D. Chrissikos, Phys. Rev. B 60 (1999) 3885–3898.
[11] E.I. Kamitsos, G.D.J. Chryssicos, Mol. Struct. 247 (1991) 1–16.
[12] A. Ivankov, J. Seekamp, W.J. Bauhofer, Luminescence 121 (2006) 123–131.
[13] S.W.S. McKeever, Thermoluminescence of Solids, Cambridge University Press, Cambridge, 1985.
[14] N.P. Lower, J.L. McRae, H.A. Feller, A.R. Betzen, S. Kappor, M. Affatigato, S.A. Feller, J. Non-Cryst. Solids 293–295 (2001) 669–675.
[15] N.A. Toropov, Handbook of phase diagram of silicate systems, Binary Systems, vol. 1, Nauka Press, Leningrad, 1972.
[16] M.L.F. Nascimento, L.A. Souza, E.B. Ferreira, E.D.J. Zanotto, Non-Cryst. Solids 351 (2005) 3296–3308.
[17] I. Avramov, E.D. Zanotto, M.O.J. Prado, Non-Cryst. Solids 320 (2003) 9–20.
[18] C.N. Santos, D.S. Meneses, P. Echeugt, D.R. Neuville, A.C. Hernandes, A. Ibanez, Appl. Phys. Lett. 94 (2009) 151901-1–151901-3.
[19] H. Li, Y. Su, L. Li, D.M.J. Strachan, Non-Cryst. Solids 292 (2001) 167–176.
[20] D. Maniu, T. Iliescu, I. Ardelean, S. Cinta-Pinzaru, N. Tarcea, W.J. Kiefer, Mol. Struct. 651 (2003) 485–488.
[21] A. Winterstein-Beckmann, D. Möncke, D. Palles, E.I. Kamitsos, L.J. Wondraczek, Non-Cryst. Solids 376 (2013) 165–174.
[22] E.J. Mansour, Non-Cryst. Solids 357 (2011) 1364–1369.
[23] M. Ishii, et al., Radiat. Meas. 38 (2004) 571–574.
[24] Binnemans K., Görller-Walrand C. Mettalurgical Industry Press, 198-201 (1995).